Macromolecules
ARTICLE

Macromolecules **2009**, *42*, 7811–7819 **7811**
DOI: 10.1021/ma901338v

Enzymatic Synthesis and Structural and Thermal Properties of Poly(ω-pentadecalactone-*co*-butylene-*co*-succinate)

Laura Mazzocchetti and Mariastella Scandola*

Department of Chemistry "G. Ciamician" and INSTM UdR Bologna, University of Bologna, via Selmi 2, 40126 Bologna, Italy

Zhaozhong Jiang*

Biomedical Engineering Department, Yale University, 55 Prospect Street, New Haven, Connecticut 06511

Received June 22, 2009; Revised Manuscript Received September 7, 2009

ABSTRACT: Poly(ω-pentadecalactone-*co*-butylene-*co*-succinate) copolymers with various compositions were synthesized via copolymerization of dialkyl succinate with 1,4-butandiol and ω-pentadecalactone (PDL) catalyzed by immobilized *Candida antarctica* lipase B. The monomer unit ratio in the copolymers can be carefully controlled by adjusting monomer feed ratio. NMR spectroscopy shows that the copolymers have nearly random distribution of PDL, butylene, and succinate repeat units, linked by ester groups along the macromolecule. Thermal stability of poly(PDL-*co*-butylene-*co*-succinate)s is composition-dependent and increases with increasing PDL unit content. All copolymers are highly crystalline irrespective of their composition, and they show isodimorphic behavior, with the crystal lattices of poly(ω-pentadecalactone) and of poly(butylene succinate) being capable of hosting foreign comonomer units up to a given extent. The two types of crystals are stable in different composition ranges. The T_m/composition dependence shows a minimum at 35 mol % PDL (pseudoeutectic composition), where PBS-type and PPDL-type crystals coexist. Cocrystallization with high extent of comonomer inclusion is supported by application of the Wendling–Suter model to the experimental T_m values. Nanoparticles prepared from these copolymers maintain a high crystallinity degree associated with isodimorphic behavior.

Introduction

Aliphatic polyesters are important biodegradable materials, and a number of such polymers, including poly(glycolide), poly(lactide), poly(glycolide-*co*-lactide), and poly(*p*-dioxanone), have been extensively used in biomedical applications.[1−3] They are primarily produced through condensation polymerization of aliphatic dicarboxylic acids (or diesters) with diols, polymerization of hydroxy acids, and ring-opening polymerization of lactones.[4]

Synthesis of aliphatic polyesters using enzyme as catalyst is particularly beneficial to provide metal-free, high-purity, medical grade polyesters due to high selectivity of enzyme catalysts.[5−11] Enzymatic syntheses of poly(butylene succinate) (PBS),[12] poly(ω-pentadecalactone) [poly(PDL)],[13−15] and relevant copolymers[14,16−22] have been recently reported in the literature. Chemically produced PBS is available commercially from Showa Highpower Co., Ltd. As a typical example of aliphatic lactone−diester−diol copolymers, poly(PDL-*co*-butylene-*co*-succinate) is especially interesting since the copolymer is expected to exhibit tunable physical properties, intermediate between those of poly(PDL) and PBS. Worth noting is that, although presently oil-derived, butylene and succinate units precursors can be obtained from renewable sources,[23] increasing the interest toward these biodegradable polyesters. In addition, complete hydrolytic degradation of poly(PDL-*co*-butylene-*co*-succinate) would only generate nontoxic byproducts: ω-hydroxy fatty acid, succinic acid, and 1,4-butanediol. The anticipated slower biodegradation rates of poly(PDL-*co*-butylene-*co*-succinate) copolymers vs poly(glycolide) and poly(glycolide-*co*-lactide) could render them suitable as bioresorbable materials for surgical applications in repairing dysfunctional digestive organs. Indeed, fast-degrading polyesters, including poly(glycolide), poly(glycolide-*co*-lactide), and poly(*p*-dioxanone), would have a substantially short service life in low-pH environments (e.g., at pH ≈ 2 in stomach) and/or in the presence of various hydrolases (e.g., pancreatic lipases) and could be completely degraded before surgical wounds are healed.

In the previous studies on enzymatic synthesis of polyesters, the polymer products were prepared via ring-opening polymerization of lactones, polycondensation of diacids (or diesters) with diols, or polymerization of hydroxy acids.[24] Enzymatic synthesis of aliphatic lactone−diester−diol copolymers was previously reported using divinyl diesters as comonomers and various lipases as catalysts.[25] The formed copolyesters had nonrandom repeating unit arrangement in the polymer chains. Recently, Jiang reported[26] successful preparation of poly(PDL-*co*-butylene-*co*-succinate) copolymers through copolymerization of conventional monomers [ω-pentadecalactone (PDL), diethyl succinate (DES), and 1,4-butanediol (BD)] using *Candida antarctica* lipase B (CALB) as catalyst (Scheme 1). The lactone−diester−diol copolymerization method employs dialkyl diester as a comonomer instead of expensive and chemically unstable divinyl diester earlier used by Namekawa et al.[25] Owing to intrinsically different reaction equilibria when using dialkyl diester instead of divinyl diester in lactone−diester−diol terpolymerization, the products formed from the two reactions possess different microstructure. Indeed, comonomer unit distribution in lactone−dialkyl diester−diol copolymers is nearly random.[26] Terpolymers with random comonomer distribution are expected

*Corresponding authors. E-mail: mariastella.scandola@unibo.it (M.S.); zhaozhong.jiang@yale.edu (Z.J.).

Published on Web 09/22/2009

Scheme 1. Two-Stage Process for Copolymerization of PDL, DES, and BD

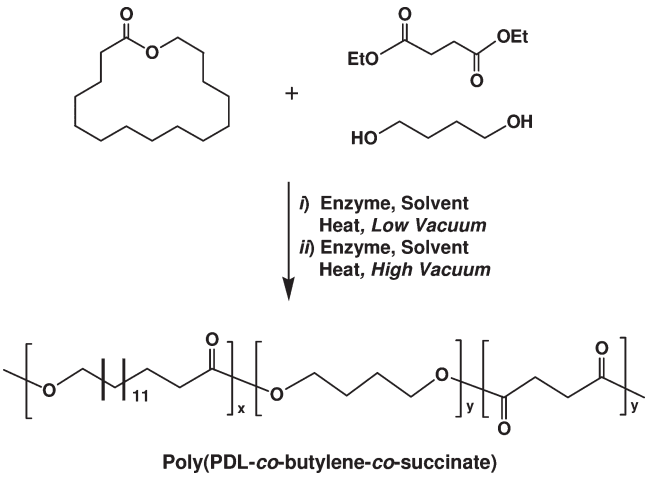

Poly(PDL-*co*-butylene-*co*-succinate)

to lead to materials whose properties may be tuned by playing on composition much more easily than the blocky polymers earlier obtained by Namekawa[25] starting from lactone−*divinyl diester*−diol.

The PDL−DES−BD copolymerization, studied at 1:1:1 monomer molar ratio and changing polymerization conditions,[26] yielded poly(PDL-*co*-butylene-*co*-succinate) copolymers containing equal moles of PDL, butylene, and succinate repeat units, with M_w up to 77 000 and M_w/M_n between 1.7 and 4.0.

This paper reports the synthesis of poly(PDL-*co*-butylene-*co*-succinate)s with different ratios of PDL to succinate units as well as their molecular and solid-state characterization. The nature of the polycondensation reaction dictates that DES-to-BD feed molar ratio has to be kept strictly at 1:1 in order to synthesize high molecular weight polymers. The ratio of PDL to DES (or BD) was adjusted systematically to form poly(PDL-*co*-butylene-*co*-succinate) copolymers with various PDL/succinate (or PDL/butylene) unit ratios. Experiments were also performed to study the effects of PDL/DES monomer ratio on the polymerization rate, composition (repeat unit ratio), molecular weight averages, and polydispersity of obtained polymers. Finally, nanoparticles were fabricated from the synthesized poly(PDL-*co*-butylene-*co*-succinate)s, whose size distribution and solid-state properties are reported.

Experimental Section

Materials. Diethyl succinate (DES), 1,4-butanediol (BD), ω-pentadecalactone (PDL), and diphenyl ether were purchased from Aldrich Chemical Co. in the highest available purity and were used as received. Immobilized CALB (*Candida antarctica* lipase B supported on acrylic resin, Novozym 435), chloroform (HPLC grade), chloroform-*d*, and methanol (98%) were also obtained from Aldrich Chemical Co. The lipase catalyst was dried at 50 °C under 2.0 mmHg for 20 h prior to use. Poly(ω-pentadecalactone) (PPDL: M_w = 64 400, M_w/M_n = 2.2) was synthesized following a procedure analogous to that reported in ref 14, except that the reaction temperature and time were 80 °C and 24 h, respectively. Poly(butylene succinate) (PBS: M_w = 32 000, M_w/M_n = 2.3) was prepared according to the procedure described in ref 16 and was subsequently purified via solubilization in $CHCl_3$ and precipitation in CH_3OH.

Instrumental Methods. ^1H and ^{13}C NMR spectra were recorded on a Bruker AVANCE 500 spectrometer. The chemical shifts reported were referenced to internal tetramethylsilane (0.00 ppm) or to the solvent resonance at the appropriate frequency. The number- and weight-average molecular weights (M_n and M_w, respectively) of polymers were measured by gel permeation chromatography (GPC) using a Waters HPLC system equipped with a model 1515 isocratic pump, a 717 plus autosampler, and a 2414 refractive index (RI) detector with Waters Styragel columns HT6E and HT2 in series. Empower II GPC software was used for running the GPC instrument and for calculations. Both the Styragel columns and the RI detector were heated and maintained at 40 °C during sample analysis. Chloroform was used as the eluent, and polymer molecular weights were determined based on a conventional calibration curve generated by narrow polydispersity polystyrene standards from Aldrich Chemical Co. Thermogravimetric (TGA) measurements were carried out using a TA-TGA 2950. The analyses were performed at 10 °C/min from room temperature to 600 °C under nitrogen flow. Differential scanning calorimetry (DSC) measurements were performed using a TA DSC-Q100 apparatus, equipped with a liquid nitrogen cooling system (LNCS) accessory. Heating scans were run at 20 °C/min from −90 to 180 °C in a helium atmosphere. Between heating scans, either constant rate cooling (10 °C/min) or quench cooling was applied. Crystallization temperature (T_c) and melting temperature (T_m) were taken at the peak maximum of endotherm and exotherm, respectively. In the presence of multiple endotherms, the temperature of the most intense peak was taken as T_m. Wide-angle X-ray diffraction measurements (WAXS) were carried out at room temperature with a PANalytical X'Pert PRO diffractometer equipped with an X'Celerator detector (for ultrafast data collection). A Cu anode was used as X-ray source (Kα radiation: λ = 0.154 18 nm, 40 kV, 40 mA), and 1/4° divergence slit was used to collect the data in 2θ range from 2° to 60°. Real-time XRD patterns were collected at different temperatures up to 80 °C by using an Anton Paar TTK450 heating device. The procedure was the following: a heating scan was run at 5 °C/min and was stopped at selected temperatures, where XRD curves were collected in isothermal mode. In order to reduce duration of isothermal data collection, the 2θ range was reduced to 15−35°, and 1° divergence slit was used to maximize incident X-ray beam. Each isothermal collection lasted about 40″, and then the heating run was resumed. After subtracting the diffractogram of an empty sample holder from the experimental diffraction curve, the amorphous and crystalline contributions in the resulting diffractogram were calculated by a fitting method using the Fityk software. The degree of crystallinity (χ_c) was evaluated as the ratio of the crystalline peak areas to the total area under the scattering curve. Isothermal crystallization experiments were performed as follows. A small amount of copolymer was inserted between two microscope cover glasses that were placed in the hot stage (Linkham TH600) of a polarizing optical microscope (OM, Zeiss Axioscop) and heated at 20 °C/min to 170 °C (i.e., well above the melting temperature). Then a gentle pressure was applied to the upper glass to squeeze the melt into a thin film, and the temperature was rapidly lowered (cooling rate >250 °C/min) to the selected crystallization temperature (T_c = 65 °C). Crystallization was allowed to proceed for 200 min, and then the sample was cooled to room temperature. Pictures were digitally acquired with a AxioCam MRc (Zeiss) camera. The Zeiss AxioVision 3.0 software was used for image analysis. Dynamic mechanical (DMTA) measurements were carried out on hot pressed rectangular films (40 mm × 8 mm, average thickness = 220 μm) in tensile mode, at 3°/min and 3 Hz from −150 to 10 °C, using a DMTA MkII (Polymer Laboratories Ltd.). Surface morphology and size of nanoparticles were analyzed using a XL30 ESEM scanning electron microscope (FEI Co.). Particle samples were mounted on an aluminum stub using carbon adhesive tape and were sputter-coated with a mixture of gold and palladium (60:40) under low-pressure argon using a Dynavac Mini Coater. The image-analysis application program, ImageJ (developed by Wayne Rasband, NIH), was used to measure particle diameters, to calculate average particle sizes, and to determine particle size distributions.

CALB-Catalyzed Copolymerization of ω-Pentadecalactone (PDL), Diethyl Succinate (DES), and 1,4-Butanediol (BD). The copolymerizations were catalyzed by 10 wt % Novozym 435

Table 1. Effect of Monomer Ratio and Reaction Time on Copolymerization[a] of ω-Pentadecalactone (PDL), Diethyl Succinate (DES), and 1,4-Butanediol (BD)

			copolymer		
sample	reaction time (h)[b]	PDL/DES/BD (molar ratio)	P/S/B[c] unit ratio[d]	M_w[e]	M_w/M_n[e]
A-20PDL	4	20:80:80		15 900	2.1
A-20PDL	8	20:80:80		26 900	2.6
A-20PDL	24	20:80:80		71 600	2.4
A-20PDL	51	20:80:80	19:81:81	106 000	2.5
A-40PDL	4	40:60:60		22 500	2.1
A-40PDL	8	40:60:60		39 700	2.6
A-40PDL	24	40:60:60		74 800	3.0
A-40PDL	51	40:60:60	39:61:61	75 000	3.4
A-60PDL	4	60:40:40		28 000	2.3
A-60PDL	8	60:40:40		53 000	2.5
A-60PDL	24	60:40:40		89 200	2.3
A-60PDL	51	60:40:40	60:40:40	90 700	2.6
A-80PDL	4	80:20:20		33 500	2.1
A-80PDL	8	80:20:20		55 200	2.1
A-80PDL	24	80:20:20		82 000	2.2
A-80PDL	51	80:20:20	81:19:19	87 600	2.5

[a] Conditions: in diphenyl ether; 10 wt % Novozym 435 vs total monomer; first stage oligomerization: 95 °C, 600 mmHg, 20 h; second stage polymerization: 95 °C, 1.8 mmHg, 51 h. [b] Reaction time of the second stage polymerization. [c] Unit abbreviations: P for ω-pentadecalactone unit; B for butylene unit; S for succinate unit. [d] Calculated from the proton NMR spectra. [e] Measured by GPC.

Table 2. Yield, Composition, Molecular Weight, and Polydispersity of Purified Poly(PDL-*co*-butylene-*co*-succinate) Copolymers

			copolymer		
sample	PDL:DES:BD[a] (feed)	polymer yield (%)	P:S:B[b] unit ratio[c]	M_w[d]	M_w/M_n[d]
P-20PDL	20:80:80	94	20:80:80	103 000	3.8
P-35PDL	35:65:65	92	35:65:65	101 000	3.4
P-50PDL	50:50:50	95	50:50:50	85 400	3.5
P-65PDL	65:35:35	94	65:35:35	100 000	3.5
P-79PDL	79:21:21	93	79:21:21	91 100	2.3

[a] Molar ratio. [b] Unit abbreviations: P for ω-pentadecalactone unit; B for butylene unit; S for succinate unit. [c] Calculated from ^{1}H NMR spectra of the copolymers. [d] Measured by GPC.

(vs total monomer) in diphenyl ether (200 wt % vs total monomer) using a parallel synthesizer connected to a vacuum line with the pressure (±0.2 mmHg) controlled by a digital vacuum regulator. The adopted PDL:DES:BD monomer molar ratios are shown in Table 1. All polymerization reactions were performed at 95 °C using a two-stage process: first stage was an oligomerization carried out under 600 mmHg pressure for 20 h, and it was followed by a second stage polymerization under 1.8 mmHg pressure for 51 h. To monitor polymer chain growth, aliquots were withdrawn for analysis at different time intervals (4, 8, 24, and 51 h) during the second stage polymerization. The copolymers are labeled as A-*x*PDL, where *x* is the percentage molar ratio of PDL vs (PDL + DES) monomers, and the letter A indicates polymer in aliquots. The aliquot samples were dissolved in HPLC-grade chloroform, and the resultant chloroform solutions were filtered to remove the enzyme catalyst.

Products were not fractionated by precipitation prior to analysis of molecular weight and structure. The filtrates containing whole products were analyzed by GPC. To determine polymer structures, aliquots were dissolved in chloroform-*d*. The resultant chloroform-*d* solutions were filtered to remove catalyst particles and were analyzed by ^{1}H and ^{13}C NMR spectroscopy. Copolymer composition (repeating unit ratio), weight-average molecular weight, and polydispersity index are reported in Table 1.

Synthesis and Purification of Poly(PDL-*co*-butylene-*co*-succinate) Copolyesters for Thermal Characterizations. Five poly(PDL-*co*-butylene-*co*-succinate) copolymers were synthesized following a procedure analogous to the one described above. Monomer feeds employed are shown in Table 2. The first-stage oligomerizations were operated at 95 °C under 600 mmHg for 18 h, and the subsequent second-stage polymerizations were carried out at 95 °C under 2.0 mmHg for 48 h. At the end of the reactions, each product mixture was dissolved in chloroform, and the resultant chloroform solution was filtered to remove the enzyme catalyst. After being concentrated under vacuum, the filtrate was dropwise added to stirring methanol to cause precipitation of a white solid polymer. The obtained precipitate was then filtered, washed with methanol three times, and dried under vacuum at 30 °C overnight. These copolymers are labeled P-*x*PDL, where *x* is the percentage molar ratio of PDL vs (PDL + DES) monomers and P indicates that polymer samples have been purified. The yield, composition, molecular weight (M_w), and polydispersity of the five isolated poly(PDL-*co*-butylene-*co*-succinate) copolymers are summarized in Table 2.

Preparation of Poly(PDL-*co*-butylene-*co*-succinate) Nanoparticles. The nanoparticles were fabricated using an oil-in-water single emulsion technique. In a typical experiment, 100 mg of poly(PDL-*co*-butylene-*co*-succinate) was dissolved in 2 mL of methylene chloride in a glass tube. The resultant organic solution was dropwise added to 4 mL of 5 wt % PVA aqueous solution while vortexing. The mixture was subsequently sonicated three times (with each time lasting for 10 s) with a TMX 400 sonic disruptor (Tekmar, Cincinnati, OH) to yield a homogeneous oil-in-water emulsion. This emulsion was immediately poured into 100 mL of aqueous solution containing 0.3 wt % PVA, and the whole mixture was magnetically stirred in an open beaker at room temperature for 3 h. This process allows nanoparticles to form via gradual evaporation of the methylene chloride solvent. The formed nanoparticles were collected by centrifugation at 11000*g* for 15 min, washed three times with deionized water, and then dried in a lyophilizer.

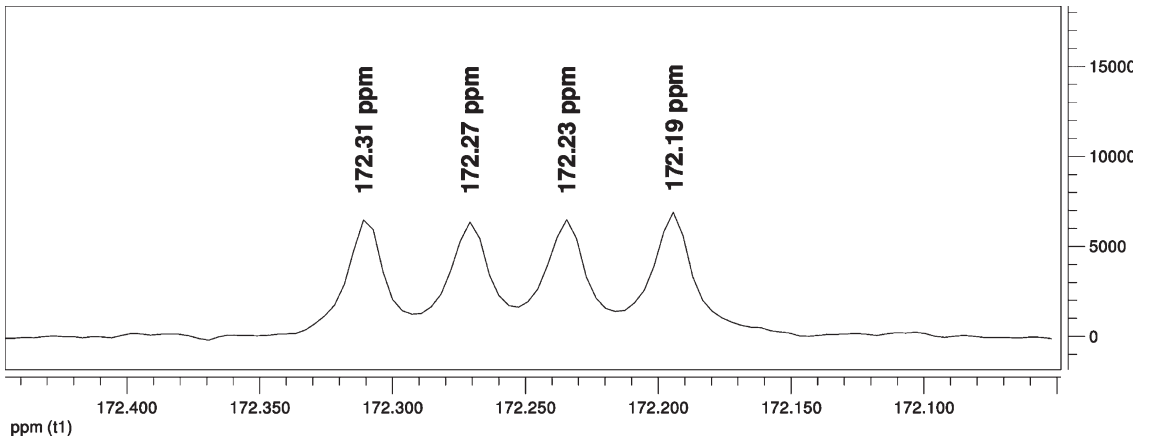

Figure 1. Expanded ^{13}C NMR spectrum showing carbonyl resonance absorptions of different succinate units in P-65PDL: absorbances at 172.31, 172.27/172.23, and 172.19 ppm are due to PDL−succinate*−PDL, PDL−succinate*−butylene (or butylene−succinate*−PDL), and butylene−succinate*−butylene triads, respectively.

Table 3. Relative Distributions of Selected Triads for Poly(PDL-*co*-butylene-*co*-succinate) Copolymers

		P-S*-P[a]		P-S*-B + B-S*-P[a]		B-S*-B[a]	
sample	copolymer unit ratio: P:B:S[a]	meas[b]	calc[c]	meas[b]	calc[c]	meas[b]	calc[c]
P-20PDL	20:80:80	1	1	17.8	16.5	64.5	65.8
P-35PDL	35:65:65	1	1	7.5	7.4	13.6	13.8
P-50PDL	50:50:50	1	1	4.0	4.0	3.8	4.0
P-65PDL	65:35:35	1	1	2.2	2.2	1.3	1.2
P-79PDL	79:21:21	1	1	1.1	1.1	0.28	0.28

[a] Unit abbreviations: P for ω-pentadecalactone unit; B for butylene unit; S for succinate unit. [b] Measured from the ^{13}C NMR spectra. [c] Calculated for a random poly(PDL-*co*-butylene-*co*-succinate) copolymer; the numbers are relative distributions of X-S*-Y (X and Y independently equal to P or B) triads vs that of P-S*-P in the polymer chains; distribution of X-S*-Y = $f_X \times f_Y$ (f_X and f_Y independently equal to f_P or f_B; f_P = molar fraction of P units in the chains; f_B = 2 × molar fraction of B units in the chains).[25]

Results and Discussion

Effects of Monomer Feed Ratio on Copolymerization of PDL, DES, and BD. The synthesis and detailed structural characterization of PDL−DES−BD copolymers with 1:1:1 PDL/succinate/butylene unit ratio was the subject of a separate publication.[26] Current studies were conducted to explore the synthesis of PDL−DES−BD copolymers with compositions other than 1:1:1 molar ratio of PDL to succinate to butylene units. The monomer ratio in the feeds was varied to check its effects on polymerization rate and on resultant copolymer molecular weight and composition. The adopted feed compositions are reported in Table 1 along with weight-average molecular weight and polydispersity index of the products formed at different reaction times. PDL comonomer was completely reacted at the end of the first stage oligomerization reactions. Thus, subsequent chain growth takes place predominantly via polycondensation reactions. For all reactions during initial 24 h of polymerization in the second stage, polymer chains grew rapidly, and polymer molecular weight increase was faster for A-60PDL and A-80PDL than for A-20PDL and A-40PDL. This is true also for the samples withdrawn after 4 and 8 h of reaction (Table 1). After 24 h, chain growth substantially slows down with the exception of A-20PDL. The copolymerization reaction for A-20PDL continued at a significant rate from 24 to 51 h to form the highest molecular weight copolymer. A possible explanation for the observed continuing chain growth is that in this particular case both ethyl ester and hydroxyl end groups are still present in near equal amounts after 24 h during the reaction. The polymer chain growth would surely stop when either ethyl ester end groups or hydroxyl termini are completely reacted. Polydispersities of all copolymers were between 2.1 and 2.6, except two high molecular weight (M_w > 74 000 Da) A-40PDL products, which have M_w/M_n values in the range from 3.0 to 3.4.

The copolymer microstructures were analyzed using both ^1H and ^{13}C NMR spectroscopy, details of which have been reported in a separate publication.[26] The compositions of the copolymers, which contain PDL, butylene, and succinate repeating units, were measured by ^1H NMR spectroscopy. As reported in Table 1, comparison between the monomer feed ratios (molar ratios of PDL:DES:BD) and copolymer compositions (molar ratios of PDL:succinate:butylene units) shows that they are in excellent agreement with what might be expected based on the monomer feed. Thus, the poly(PDL-*co*-butylene-*co*-succinate) copolymer composition can be easily controlled by using an appropriate monomer feed ratio.

Preparation of Purified Poly(PDL-*co*-butylene-*co*-succinate) Copolyesters for Solid State Characterization. The synthesized copolymers were purified via solubilization/precipitation in $CHCl_3/CH_3OH$ after removal of the catalyst particles at the end of the reactions. Table 2 summarizes the yield, composition, molecular weight (M_w), and polydispersity of the five isolated poly(PDL-*co*-butylene-*co*-succinate) copolymers. As shown in the table, the copolymers were obtained in good yields (92−95%) with M_w ranging from 85 000 to 103 000 and M_w/M_n between 2.3 and 3.8. Furthermore, the copolymer compositions match remarkably well the corresponding monomer feed ratios employed.

^{13}C NMR analysis has been proved to be effective in determining the repeating unit sequence distributions in the macromolecular chains.[26] Figure 1 displays the carbonyl ^{13}C resonance absorptions of different succinate units in P-65PDL, as an example. The absorbances at 172.31, 172.27/172.23, and 172.19 ppm are attributed respectively

Table 4. Thermal Properties of Poly(PDL-*co*-butylene-*co*-succinate) Copolymers

				DSC						DMTA
sample	PDL[a] (mol %)	PDL[b] (wt %)	T_{deg}[c] (°C)	T_c (°C)	ΔH_c (J/g)	T_m (°C)	ΔH_m (J/g)	χ_c[d]	ε/RT[e]	T_α[f] (°C)
PBS	0	0	390	74	73	113	77	59	n.d.	−34[g]
P-20PDL	20	26	402	55	58	92	51	47	0.0120	−37
P-35PDL	35	43	406	39	76	75, 56	65[h]	52	n.d.	−35
P-50PDL	50	58	408	48	91	64	88	54	0.0043	−33
P-65PDL	65	72	417	59	107	72	107	59	0.0044	−29
P-79PDL	79	84	421	68	121	81	121	64	0.0043	−23
PPDL	100	100	430	81	155	93	147	65	n.d.	−27[i]

[a] PDL molar percentage content calculated as: P/(P + S). Unit abbreviations: P is for ω-pentadecalactone unit; B for butylene unit; S for succinate unit. [b] PDL weight percentage content calculated as P/(P + S + B) where P, S and B are described at footnote *a*. [c] Measured from TGA experiments as the temperature of maximum weight loss rate. [d] Crystallinity degree from WAXS (±5%). [e] Calculated from eq 3. [f] Peak temperature of main relaxation. [g] From DMTA, ref 43. [h] Total melting enthalpy of the multiple-peak endotherm. [i] From DSC, ref 17.

to PDL−succinate*−PDL (P-S*-P), PDL−succinate*−butylene (P-S*-B)/butylene−succinate*−PDL (B-S*-P), and butylene−succinate*−butylene (B-S*-B) triad structures.[26] By integrating corresponding absorptions, the ratios of P-S*-P to (P-S*-B + B-S*-P) to B-S*-B triads were obtained for the five purified copolymers with various unit ratios, and the results are shown in Table 3. On the other hand, at a given composition, relative distributions of P-S*-P, P-S*-B, B-S*-P, and B-S*-B triads can also be calculated for statistically random poly(PDL-*co*-butylene-*co*-succinate) copolymers.

Table 3 additionally lists the calculated P-S*-P/(P-S*-B + B-S*-P)/B-S*-B triad ratios for the random copolymers P-20PDL, P-35PDL, P-50PDL, P-65PDL, and P-79PDL. Comparison between the theoretically calculated values and the experimental data clearly indicates that all five poly(PDL-*co*-butylene-*co*-succinate) copolymers have nearly random distributions of PDL, butylene, and succinate units, which are connected via ester linkages in the macromolecules.

Solid-State Characterization. Thermal properties, structure, and morphology of poly(PDL-*co*-butylene-*co*-succinate) copolymers and of reference homopolymers were investigated by TGA, DSC, WAXS, OM, and DMTA. Thermogravimetric analysis (curves not shown) reveals that thermal stability of poly(PDL-*co*-butylene-*co*-succinate) increases with increasing PDL content, i.e., with insertion of PDL units in the PBS chain.

The main weight loss step in the copolymers (Table 4) gradually shifts from 390 °C (PBS homopolymer) to 430 °C (PPDL homopolymer).

The DSC curves of all copolymers and of the reference homopolymers, obtained in controlled cooling runs from the melt and in subsequent heating scans, are displayed in Figure 2. This experimental procedure was adopted in order to erase previous thermomechanical history in all samples. In Figure 2A the two homopolymers are seen to crystallize in the same temperature range, while copolymers display composition-dependent exothermal phenomena, located at lower temperatures than those of both PBS and PPDL. The enthalpy associated with crystallization, notably higher in PPDL than in PBS, changes with composition as reported in Table 4. Upon reheating (Figure 2B), PPDL shows a sharp melting endotherm (T_m = 93 °C) while PBS exhibits cold crystallization preceding a multiple melting endotherm (main peak at 113 °C). All copolymers rich in PDL units (i.e., ≥50 mol %, Figure 2B: curves d−f) show a sharp endotherm reminiscent of that of PPDL, whose temperature decreases with increasing BS content. A peculiar melting behavior is shown by P-35PDL (curve c), where a sharp peak, whose temperature location follows the PDL-rich copolymers trend, is followed by a broader one. The succinate-richest copolymer (P-20PDL, curve b) melts in a temperature range higher than P-35PDL but lower than homopolymer PBS.

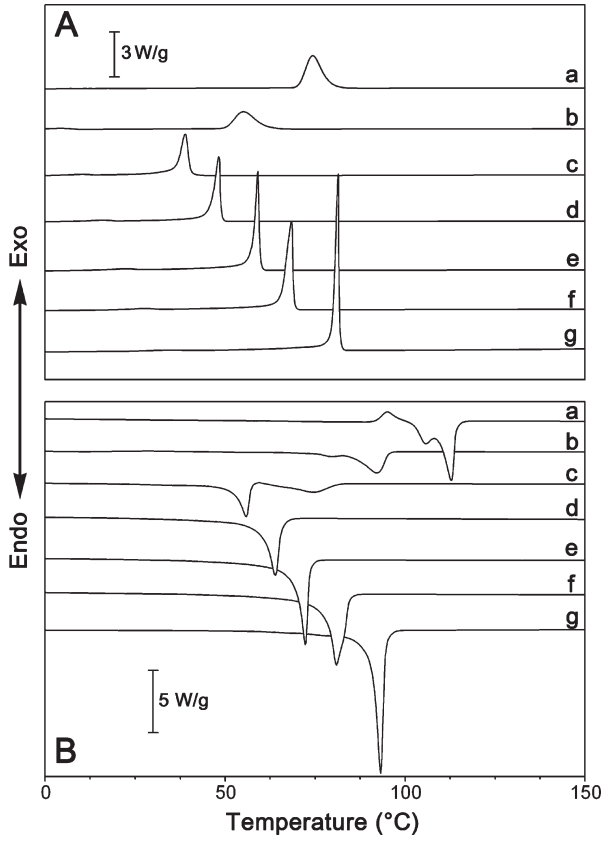

Figure 2. DSC thermograms of a cooling scan from the melt at 10°/min rate (A) and of a subsequent heating run at 20°/min (B) of poly(PDL-*co*-butylene-*co*-succinate)s and of reference homopolymers: (a) PBS; (b) P-20PDL; (c) P-35PDL; (d) P-50PDL; (e) P-65PDL; (f) P-79PDL; (g) PPDL.

Crystallization and melting temperatures (from DCS) are plotted in Figure 3A as a function of copolymer composition. While PPDL exhibits a quite small undercooling ($T_m - T_c$ ca. 20 °C), that of PBS is much larger (ca. 40 °C). Notably, PDL-rich copolymers maintain the same extent of undercooling as PPDL, while in P-20PDL the difference between T_m and T_g well compares with that of PBS. Copolymer P-35PDL shows a single exothermal event upon cooling (Figure 2A), whose T_c lays at the convergence of the T_c−composition dependences of PDL-rich and BS-rich copolymers (Figure 3A). The two endotherms shown by P-35PDL in the heating run (Figure 2B) remarkably well fit the two T_m−composition trends characterizing PDL-rich and BS-rich copolymers in Figure 3A.

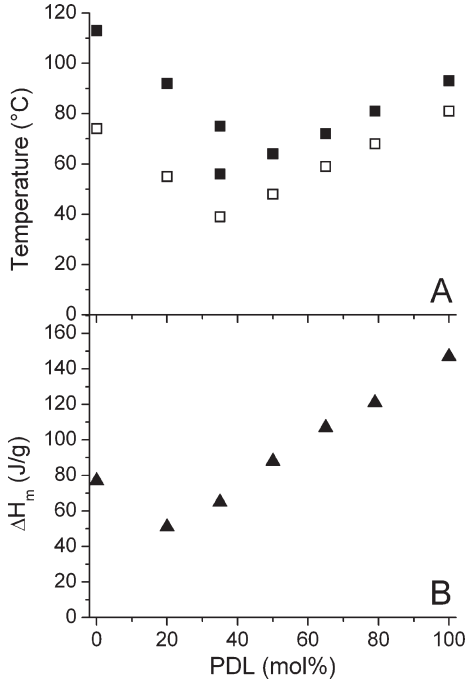

Figure 3. Composition dependence of (A) melting temperature (■) and crystallization temperature (□); (B) melting enthalpy (▲) of poly(PDL-*co*-butylene-*co*-succinate) copolymers (data in Table 4). Composition is given as PDL mol %, i.e., PDL/(PDL + succinate).

The melting enthalpy (Table 4 and Figure 3B) is high in all copolymers ($\Delta H_m \geq 51$ J/g). It shows a minimum in P-20PDL, and it increases with increasing PDL content. High melting enthalpy reflects high crystallinity, a very unusual behavior in macromolecules with random distribution of crystallizable comonomer units. This feature is particularly striking in the present system that is composed of repeating units derived from both AB type (ω-hydroxy acid) and A2 + B2 type (diacid/diester + diol) monomers. Such copolymers would normally possess a higher degree of disorder than copolymers composed of either AB monomers or A2 + B2 monomers only. Observation of high melting enthalpy in poly(PDL-*co*-butylene-*co*-succinate) copolymers, especially at intermediate compositions, suggests that in the system under investigation the counits may be able to cocrystallize, i.e., to enter—to a certain degree—the same crystal lattice.[27−31]

In order to elucidate this point, the samples were subjected to WAXS analysis. Figure 4 shows the diffractograms of copolymers and reference homopolymers, while the crystallinity degrees, calculated from the curves, are listed in Table 4. In agreement with the high melting enthalpy derived from DSC measurements, the crystallinity degree is higher than 47% in all copolymers. The diffractograms of PPDL and PBS substantially differ, reflecting the different crystal lattices in which the two homopolymers crystallize [PPDL:[32] pseudo-orthorhombic monoclinic unit cell with a = 7.49(1), b = 5.034(9) Å, c = 20.00(4) Å, α = 90.06(4)°; PBS (α-form):[33] monoclinic unit cell with a = 5.23(2) Å, b = 9.12(3) Å, c = 10.90(5) Å, β = 123.9(2)°].

Analysis of the copolymer diffractograms in Figure 4 clearly shows that P-20PDL exhibits all PBS reflections (main ones indicated by solid lines). Conversely, P-50PDL, P-65PDL, and P-79PDL exhibit the reflections typical of PPDL (main ones indicated by dashed lines) with the exception of that present at 2θ = 4.52° in the homopolymer, which is indexed (001) and corresponds to a 19.54 Å periodicity in the chain direction.[32] A peculiar behavior in Figure 4 is

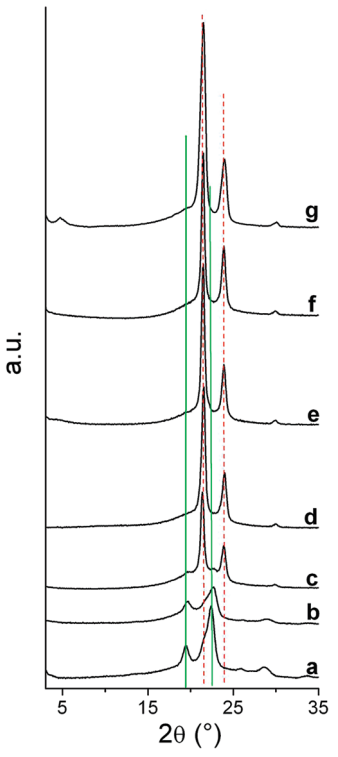

Figure 4. WAXS diffractograms of (a) PBS, (b) P-20PDL, (c) P-35PDL, (d) P-50PDL, (e) P-65PDL, (f) P-79PDL, and (g) PPDL. Typical PPDL and PBS reflections are highlighted by red (dashed) and green (solid) lines, respectively.

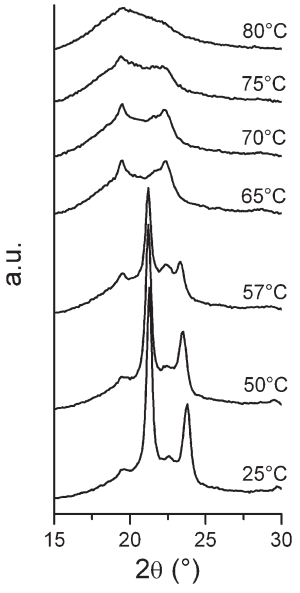

Figure 5. WAXS diffractograms of P-35PDL collected at different temperatures (indicated on curves).

displayed by copolymer P-35PDL, whose diffractogram contains both PBS and PPDL reflections. At either side of this particular composition (i.e., at higher or lower PDL content) only one crystal lattice develops.

WAXS diffractograms of P-35PDL, collected at increasing temperatures (Figure 5), show sequential disappearance of PPDL and of PBS reflections at temperatures close to the T_ms observed by DSC (see Figure 2B), thus confirming that the two melting events displayed by this copolymer (at 56 and 75 °C) underlie the presence of the two mentioned crystal

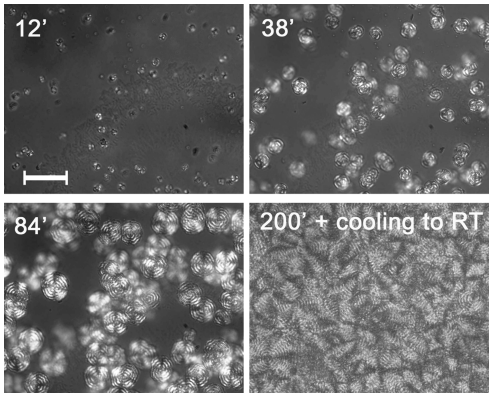

Figure 6. Polarized optical micrographs of P-35PDL during isothermal crystallization from the melt at 65 °C. Pictures were taken after the time indicated on each image. The last picture refers to the morphology obtained after 200′ at 65 °C followed by cooling to RT. Scale bar (common to all pictures) is 50 μm.

phases. If the copolymer is allowed to isothermally crystallize in between the two T_ms of P-35PDL, i.e., at 65 °C, banded spherulites, reminiscent of those of plain PBS, are seen to grow at a constant rate and eventually to impinge, as illustrated in Figure 6.

Upon subsequent cooling of the sample from 65 °C to room temperature, an increase of spherulite birefringence is observed. WAXS analysis of this sample confirms the presence of both PPDL and PBS crystal lattices, with a larger contribution of the PBS phase compared with the nonisothermally crystallized copolymer. In agreement with such results, DSC analysis (curve not reported) of P-35PDL isothermally crystallized at 65 °C shows changes of relative peak intensity in the multiple endotherm characterizing this copolymer. Indeed, a rough estimate of the melting enthalpies of the individual processes yields 30 J/g (PPDL) vs 34 J/g (PBS) after isothermal crystallization at 65 °C to be compared with 43 J/g (PPDL) vs 22 J/g (PBS) after crystallization during controlled cooling at 10 °C/min in the DSC.

Random copolymers showing high crystallinity over the whole composition range, and exhibiting the crystal phase of either homopolymer, depending on the composition region, are known in the literature as isodimorphic systems.[27−31,34] In such systems the crystal lattice of each homopolymer is capable of hosting foreign comonomer units up to a given extent. Isodimorphic copolymers are expected to show a change from one lattice to the other at a given composition—typical of each system—where both phases can coexist. The T_m of each crystal phase reaches a minimum at such composition that, therefore, is named the pseudoeutectic. In poly(PDL-*co*-butylene-*co*-succinate) the pseudoeutectic composition is that of copolymer P-35PDL (Figure 3A), where PPDL-type and PBS-type crystals develop side by side.

Earlier evidence of cocrystallization in random copolymers of PDL with caprolactone (CL)[35] has been reported in the literature. Such system showed isomorphic substitution of comonomer units, promoted by high similarity of the homopolymers' unit cells [poly-ε-caprolactone:[36] orthorhombic with a = 7.496, b = 4.974 Å, and c (fiber axis) = 17.297 Å]. In poly(PDL-*co*-CL) copolymers it was observed that the PPDL (001) reflection at low 2θ angles tended to disappear with increasing CL content. This observation was attributed to disruption of the regular ester group spacing that originates the reflection at $2\theta = 4.52°$ in PPDL, upon random insertion of comonomer units in the macromolecule. An analogous explanation might hold in poly(PDL-*co*-butylene-*co*-succinate) copolymers (Figure 4), when butylene and/or succinate units enter PPDL crystals.

When a crystal phase develops in random copolymers, a melting point depression is always observed, as also found in the present system (Figure 3A). Flory first addressed this phenomenon[37,38] and provided an equation describing the decrease of T_m as a function of comonomer content, on the assumption that the foreign counits are totally excluded from the lattice of the crystallizing polymer. Later Baur[39] introduced the concept that the average length of crystallizing sequences (ξ) must be shorter in the random copolymer than in the homopolymer, if it is assumed that comonomer units cannot enter the crystals. An alternative view, taking into account the possibility that a certain amount of counits might be hosted in the crystal lattice, was earlier put forward by Helfand and Lauritzen[40] and further developed by Sanchez and Eby.[41] Hence, new equations allowing to quantify the equilibrium comonomer unit fraction included in the lattice were proposed. A later effort to combine the concept of comonomer inclusion with that of finite length of crystallizing polymer sequences led Wendling and Suter[42] to propose the following equation for the melting point depression of a random poly(A-*co*-B) copolymer:

$$\frac{1}{T_m(X_B)} - \frac{1}{T_m^0} = \frac{R}{\Delta H_m^0}\left\{\frac{\varepsilon X_{CB}}{RT_m} + (1 - X_{CB})\ln\frac{1 - X_{CB}}{1 - X_B} + X_{CB}\ln\frac{X_{CB}}{X_B} + \langle\xi\rangle^{-1}\right\} \quad (1)$$

where T_m^0 and $\Delta H_m^0$are respectively the equilibrium melting temperature and enthalpy of the poly(A) homopolymer, X_B is the copolymer composition (expressed as molar fraction of B units), $T_m(X_B)$ is the experimental copolymer melting temperature, R is the gas constant (8.314 J K^{-1} mol^{-1}), X_{CB} is the molar fraction of foreign B counits in the crystal, ε is the average defect free energy, and $\langle\xi\rangle$ is the average length of crystallizing copolymer sequences.

At equilibrium, the concentration of B counits that are included into the crystal is[41]

$$X_{CB}^{eq} = \frac{X_B e^{-\varepsilon/RT}}{1 - X_B + X_B e^{-\varepsilon/RT}} \quad (2)$$

and consequently eq 1 reduces to[42]

$$\frac{1}{T_m^0} - \frac{1}{T_m^0(X_B)} = \frac{R}{\Delta H_m^0}\{\ln(1 - X_B + X_B e^{-\varepsilon/RT}) - \langle\xi\rangle^{-1}\} \quad (3)$$

where at equilibrium $\langle\xi\rangle^{-1} = 2(X_B - X_B e^{-\varepsilon/RT})(1 - X_B + X_B e^{-\varepsilon/RT})$ and $T_m^0(X_B)$ is the equilibrium melting temperature of the copolymer with B units molar fraction X_B.

In this work eq 3 has been tentatively applied to the poly(PDL-*co*-butylene-*co*-succinate) system using, in a first approximation, the experimental melting temperatures instead of equilibrium melting temperatures. For each copolymer, ε/RT was evaluated as an adjustable parameter to best fit eq 3. The values of ε/RT obtained (Table 4) are quite low, as expected when substantial comonomer inclusion occurs.[41,42] This finding supports the foregoing discussion on isodimorphic behavior of this copolymer system. Comparison of the values in Table 4 shows that inclusion is slightly easier (lower ε/RT values) when the PPDL lattice hosts butylene and/or succinate units than in the case where the PBS lattice accepts PDL units.

In order to evaluate the glass transition temperature of these highly crystalline materials, the copolymers in the form of hot-pressed samples were analyzed by DMTA. Prior to

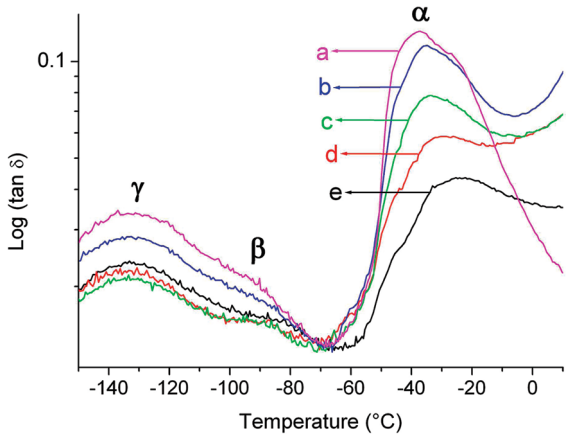

Figure 7. DMTA curves (3 Hz, 3 deg/min) of poly(PDL-*co*-butylene-*co*-succinate) copolymers: (a) P-20PDL; (b) P-35PDL; (c) P-50PDL; (d) P-65PDL; (e) P-79PDL.

DMTA measurements the hot-pressed samples were subjected to DSC analysis that yielded curves (not shown) practically identical to those in Figure 2B. The DMTA curves of all copolymers (Figure 7) display a main mechanical loss process (α-relaxation) associated with the glass transition, centered in the range from −40 to −20 °C (Table 4). Literature results show that the T_gs of the two reference homopolymers (PBS[17] and PPDL[43]) differ by a mere 10 °C and are located in the mentioned temperature range. The changes of the α relaxation observed in Figure 7 with changing composition, i.e., the slight shift to higher temperature, intensity decrease, and broadening with increasing PDL content, is mainly ascribable to a concomitant increase of crystallinity (Table 4), which contributes anchorage points to the polymer chains, through the well-known "physical cross-linking" effect.

As shown in Figure 7, the DMTA spectra of all copolymers display, in addition to the main transition (α), two low-temperature secondary relaxations (β and γ). The β relaxation, located at about −90 °C, is a so-called "diluent-induced" relaxation[44] attributed to local motions of water molecules interacting with the polar groups of the polyester macromolecule, in agreement with earlier literature concerning not only polyesters[43] but also a wide range of hydrophilic polymers.[45,46] In the DMTA curves of Figure 7 the lowest temperature mechanical loss (γ), located at about −130 °C in all poly(PDL-*co*-butylene-*co*-succinate)s regardless of their different composition, is a well-known and widely reported relaxation phenomenon, attributed to local motions of methylene sequences.[45] Both γ and β peaks are seen to decrease with increasing copolymer crystallinity, i.e., with increasing PDL content. This observation confirms that both γ and β relaxations arise from local motions in the amorphous phase.

The poly(PDL-*co*-butylene-*co*-succinate) copolymers investigated in this work were also used to produce nanoparticles (NP). The size distribution, melting point, and melting enthalpy values of the particles are summarized in Table 5. As a representative example, the SEM image of P-20PDL nanoparticles is shown in Figure 8. Thermal and structural characterization of the copolymer nanoparticles showed that they maintain the isodimorphic behavior described above for the pristine materials, with the same composition dependence of T_m, the only appreciable difference being a slightly lower melting enthalpy than that of samples crystallized under controlled cooling rate (compare Table 5 with Table 4). This result is likely due to different crystallization kinetics that during NP solidification occurs via slow solvent evaporation.

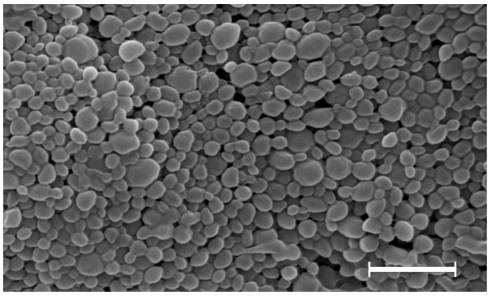

Figure 8. SEM micrograph of nanoparticles prepared from P-20PDL. Scale bar is 1 μm.

Table 5. Thermal Properties and Average Size Distribution of Poly(PDL-*co*-butylene-*co*-succinate) Nanoparticles

		DSC	
sample	ASD (nm)[a]	T_m (°C)	ΔH_m (J/g)
P-20PDL	187 ± 37	91	57
P-35PDL	209 ± 55	74, 53	74
P-50PDL	203 ± 51	63	93
P-65PDL	221 ± 59	72	105
P-79PDL	252 ± 65	80	115

[a] Average size distribution from SEM micrographs.

Conclusions

Enzymatic synthesis of poly(PDL-*co*-butylene-*co*-succinate) copolymers with various compositions was achieved via copolymerization of dialkyl succinate with BD and PDL. The unit ratio of the copolymers was readily controlled by adjusting the corresponding monomer feed ratio. The synthesized copolymers have near random distributions of PDL, butylene, and succinate repeat units. All copolymers are highly crystalline irrespective of their composition, and they show isodimorphic behavior, with the presence of PBS-type or PPDL-type crystals at either side of the pseudoeutectic composition. Application of the Wendling−Suter model suggests a high level of comonomer inclusion in both cases. This work represents, to the best of our knowledge, the first report demonstrating that isodimorphic behavior can be observed in structurally highly disordered, random copolyesters formed from AB + A2 + B2 comonomers. Highly crystalline nanoparticles were also prepared from these copolymers, whose suitability as drug carriers is currently under investigation, particularly for delivering hydrophobic anticancer drugs.

Acknowledgment. The authors thank Yale University and University of Bologna for their financial support of this work. Thanks are due to Dr. Massimo Gazzano for the high-*T* WAXS measurements and to Jie Liu for nanoparticle preparation.

References and Notes

(1) Chu, C. C. In *The Biomedical Engineering Handbook*, 2nd ed.; Bronzino, J. D., Ed.; CRC Press: Boca Raton, 2006.
(2) Kohn, J.; Langer, R. In *Biomaterials Science: an Introduction to Materials in Medicine*, Ratner, B. D., Hoffman, A. S., Schoen, F. J., Lemons, J. E., Eds.; Academic Press: New York, 1996; pp 64−72.
(3) Barrows, T. H. *Clin. Mater.* **1986**, *1*, 233–257.
(4) Odian, G. In *Principles of Polymerization*, 4th ed.; Wiley-VCH: New York, 2004.
(5) Gross, R. A.; Kumar, A.; Kalra, B. *Chem. Rev.* **2001**, *101*, 2097–2124.
(6) Kobayashi, S.; Uyama, H.; Kimura, S. *Chem. Rev.* **2001**, *101*, 3793–3818.
(7) Uyama, H.; Kobayashi, S. *Adv. Polym. Sci.* **2006**, *194*, 133–158.
(8) Matsumura, S. *Adv. Polym. Sci.* **2006**, 95–132.

(9) Jiang, Z.; Liu, C.; Xie, W.; Gross, R. A. *Macromolecules* **2007**, *40*, 7934–7943.
(10) Srivastava, R. K.; Albertsson, A. C. *Biomacromolecules* **2006**, *7*, 2531–2538.
(11) Srivastava, R. K.; Albertsson, A. C. *Macromolecules* **2006**, *39*, 46–54.
(12) Azim, H.; Dekhterman, A.; Jiang, Z.; Gross, R. A. *Biomacromolecules* **2006**, *7*, 3093–3097.
(13) Bisht, K. S.; Henderson, L. A.; Gross, R. A.; Kaplan, D. L.; Swift, G. *Macromolecules* **1997**, *30*, 2705–2711.
(14) Kumar, A.; Kalra, B.; Dekhterman, A.; Gross, R. A. *Macromolecules* **2000**, *33*, 6303–6309.
(15) Uyama, H.; Kikuchi, H.; Takeya, K.; Kobayashi, S. *Acta Polym.* **1996**, *47*, 357–360.
(16) Jiang, Z.; Liu, C.; Gross, R. A. *Macromolecules* **2008**, *41*, 4671–4680.
(17) Zini, E.; Scandola, M.; Jiang, Z.; Liu, C.; Gross, R. A. *Macromolecules* **2008**, *41*, 4681–4687.
(18) Jiang, Z.; Azim, H.; Gross, R. A.; Focarete, M. L.; Scandola, M. *Biomacromolecules* **2007**, *8*, 2262–2269.
(19) Van der Mee, L.; Antens, A.; Van de Kruijs, B.; Palmans, A. R. A.; Meijer, E. W. *J. Polym. Sci., Part A: Polym. Chem.* **2006**, *44*, 2166–2176.
(20) Magusin, P. C. M. M.; Mezari, B.; Van der Mee, L.; Palmans, A. R. A.; Meijer, E. W. *Macromol. Symp.* **2005**, *230*, 126–132.
(21) Kumar, A.; Garg, K.; Gross, R. A. *Macromolecules* **2001**, *34*, 3527–3533.
(22) Dong, H.; Wang, H. D.; Cao, S. G.; Shen, J. C. *Biotechnol. Lett.* **1998**, *20*, 905–908.
(23) Bechthold, I.; Bretz, K.; Kabasci, S.; Kopitzky, R.; Springer, A. *Chem. Eng. Technol.* **2008**, *31*, 647–654.
(24) Kobayashi, S. *Macromol. Rapid Commun.* **2009**, *30*, 237–266.
(25) Namekawa, S.; Uyama, H.; Kobayashi, S. *Biomacromolecules* **2000**, *1*, 335–338.
(26) Jiang, Z. *Biomacromolecules* **2008**, *9*, 3246–3251.
(27) Natta, G. *Makromol. Chem.* **1960**, *35*, 94–131.
(28) Natta, G.; Corradini, P.; Sianesi, D.; Morero, D. *J. Polym. Sci.* **1961**, *51*, 527–539.
(29) Allegra, G.; Bassi, I. *Adv. Polym. Sci.* **1969**, *6*, 549–574.
(30) Allegra, G.; Meille, S. V.; Porzio, W. In *Polymer Handbook*, 4th ed.; Brandrup, J., Immergut, E. H., Grulke, E. A., Eds.; Wiley-VCH: New York, 1999; pp 399−408.
(31) Wunderlich, B. In *Macromolecular Physics*; Academic Press: New York, 1973; Vol. *I*, pp 147−161.
(32) Gazzano, M.; Malta, V.; Focarete, M. L.; Scandola, M.; Gross, R. A. *J. Polym. Sci., Part B: Polym. Phys.* **2003**, *41*, 1009–1013.
(33) Ichikawa, Y.; Kondo, H.; Igarashi, Y.; Noguchi, K.; Okuyama, K.; Washiyama, J. *Polymer* **2000**, *41*, 4719–4727.
(34) Scandola, M.; Ceccorulli, G.; Pizzoli, M.; Gazzano, M. *Macromolecules* **1992**, *25*, 1405–1410.
(35) Ceccorulli, G.; Scandola, M.; Kumar, A.; Kalra, B.; Gross, R. A. *Biomacromolecules* **2005**, *6*, 902–907.
(36) Bittiger, H.; Marchessault, R. H.; Niegisch, W. D. *Acta Crystallogr., Sect. B* **1970**, *26*, 1923–1927.
(37) Flory, P. J. *J. Chem. Phys.* **1947**, *15*, 684–684.
(38) Flory, P. J. *Trans. Faraday Soc.* **1955**, *51*, 848–857.
(39) Baur, V. H. *Makromol. Chem.* **1966**, *98*, 297–297.
(40) Helfand, E.; Lauritzen, J. I. *Macromolecules* **1973**, *6*, 631–638.
(41) Sanchez, I. C.; Eby, R. K. *Macromolecules* **1975**, *8*, 638–641.
(42) Wendling, J.; Suter, U. W. *Macromolecules* **1998**, *31*, 2516–2520.
(43) Focarete, M. L.; Scandola, M.; Kumar, A.; Gross, R. A. *J. Polym. Sci., Part B: Polym. Phys.* **2001**, *39*, 1721–1729.
(44) Kolarik, J. *Adv. Polym. Sci.* **1982**, *46*, 119–161.
(45) McCrum, N. G., Read, B. E., Williams, G. In *Anelastic and Dielectric Effects in Polymeric Solids*; Dover Publications: Mineola, NY, 1991.
(46) Pizzoli, M.; Scandola, M. In *Polymeric Materials Encyclopedia*; Salamone, J. C., Ed.; CRC Press: Boca Raton, 1996.